# Palette-based Color Harmonization via Color Naming

Danna Xue, Javier Vazquez-Corral, Luis Herranz, Yanning Zhang, Michael S. Brown

*Abstract*—**Color harmony refers to combinations of colors that look pleasing together. We present a novel strategy to harmonize an image's colors using color-palette manipulation and color naming. Palette-based color manipulation is a method that extracts a few colors to represent the image. Modifying the palette colors modifies the color appearance of the image. A color-naming model is a mechanism to categorize colors into a fixed number of basic color terms. Working from a color-naming model, we derive a set of *prototype colors* and demonstrate that mapping an image's extracted color palette to the nearest prototype colors effectively harmonizes the image's colors. This straightforward approach yields visually compelling, outperforming more complex color harmony methods.**

*Index Terms*—**Color modification, color harmonization, color naming, color palette, image recoloring**

## I. INTRODUCTION AND RELATED WORK

Color modification is a crucial cornerstone in graphic design, where color coherence [1] and harmony [2] play a vital role in various applications like advertisements and brochures.

However, most methods for color manipulation focus on applying color themes to meet specific design requirements, while often overlooking the preservation of the image's natural and harmonious color composition. In this work, we take a different approach by revisiting two widely used color modification methods: palette-based image recoloring and color naming. Specifically, we demonstrate how enhancing an extracted color palette considering a color-naming model leads to more harmonious image colors. This improvement is evident compared to a method explicitly designed for color harmonization.

Palette-based color manipulation allows for intuitive adjustments of different colors, empowering designers to establish
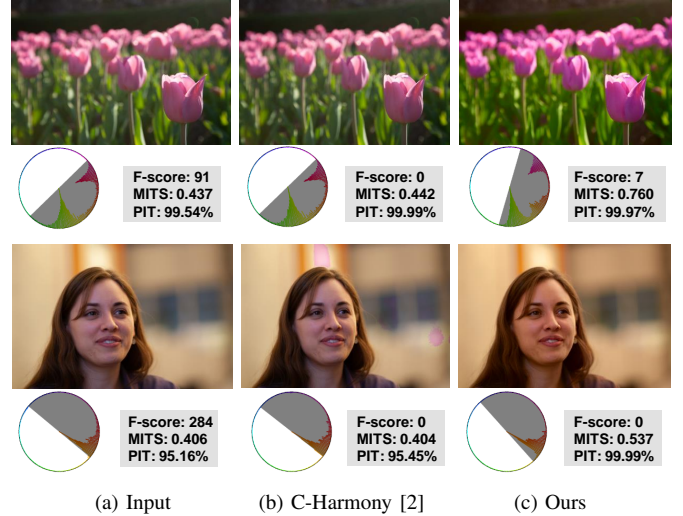
Fig. 1. Comparison between the results of color harmonization (Cohen-Or *et al.* [2]) and our approach. For each image, the optimal harmonious template (*i.e.* gray areas) on the hue wheel is shown. The collection of colors inside the gray areas is considered to be harmonious. Lower F-score and higher MITS and PIT indicate more harmonious colors. Our proposed method produces harmonized and realistic colors without few artifacts.

specific color schemes for achieving color harmony and enhancing visual appeal [1]. The process begins with palette extraction, where a set of representative colors, known as a color palette [3], is identified from an image. This palette can be manually selected [4], [5] or automatically generated using algorithms like k-means clustering [6], [7] or convex hulls [8], [9]. Once the color palette is obtained, it serves as a reference for modifying the colors in the image. Modifications may include color correction, recoloring [1], [6], [7], [10], or creating color harmonies [11].

Different from image enhancement approaches that aim to enhance colors [12]–[14], color harmonization is a technique intended to create balance and coherence among different colors within an image. Color harmonization typically follows specific color schemes to produce visually pleasing compositions. Cohen-Or *et al.* [2] have defined harmonious colors as those that adhere to a pre-defined hue distribution represented by harmonious templates. By mapping the colors in an image to this distribution using defined rules, the resulting image aligns with aesthetic design principles. Following this idea, methods have targeted improving the harmonic template search via predominant hue colors [15]–[18] or color histograms [19]. Color harmonization is a common practice used to enhance visual aesthetics, particularly in fields such as graphic design.

Color naming is the practice of associating names or labels with specific colors. The seminal work by [20] established that basic color terms that are universally recognized: *red, orange, brown, yellow, blue, pink, purple, green, black, gray, white*. Different models [21]–[24] explored how to parameterize RGB values into probabilities, which indicate the likelihood that the RGB values belong to each of these color names. Color naming categories are related to the human naming of specific objects, helping to ensure the relationship between content and colors by constraining color names.

It is important to note that both saturation and color distribution play crucial roles in achieving color harmony [2]. For this reason, we introduce the concept of color-name stability as a reference in image color adjustment. The goal is to enhance the image while maintaining its original color names. Our palette-based method achieves this by modifying color distribution to obtain a representative palette with the same color names while enhancing image saturation. This approach, unlike directly increasing overall image saturation, does not compromise color harmony. We demonstrate how the color-name stability hypothesis within an extracted palette results in an output image with harmonized image colors (see Fig. 1). Our experimental results demonstrate that our method can improve image color harmonization aesthetically and statistically.

## II. METHODOLOGY

Our approach involves four key steps: color prototype generation with color naming (II-A), color palette extraction (II-B), color matching (II-C), and palette-based image recoloring (II-D). Color prototype generation with color naming and color matching are the most crucial, as they involve deriving the new set of colors that will form the "basis" of the image. Our method mainly focuses on these steps by identifying a suitable target palette, ensuring that the recolored image based on this palette exhibits increased saturation while minimizing hue shifts. Fig. 2 shows an overview of our approach.

### A. Color Prototypes Generation with Color Naming

The objective of this step is to generate the set of candidate colors to be the prototype palettes. Our method is based on keeping the names of the colors in the palette, and therefore, we enforce that the names of the colors in the source palette are unchanged in the final target palette. To identify the color name, we apply a color-naming model [23], which assigns 11 color probabilities to any input value in the *sRGB* color space. These probabilities represent the extent to which the RGB values can be named with a specific term. We first run the color-naming model for the possible values in the whole *sRGB* color space, where $R, G, B \in [0, 255]$, with a $8 \times 8 \times 8$ grid. In this way, the color space is divided into 11 different parts, one per color term. Then, k-means clustering is applied to these color values at each part, resulting in $n$ distinct partitions per color name. Due to the varying sizes of the regions covered by different color terms, we select the number of candidate colors for each color term based on the area they cover. Specifically, we select a basic 10 colors for each term. Besides, among
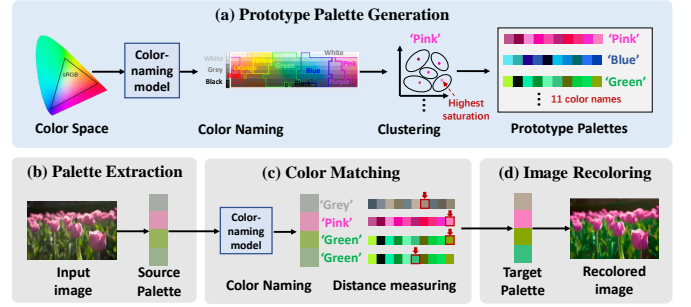


Fig. 2. The proposed palette-based color harmonization framework. All colors in the color space are categorized into 11 classes by a color-naming model, and colors with the same color name are clustered. The color with the highest saturation in each cluster is selected as a color in the prototype palettes. Given an input image, the source palette of the image is extracted. Then, the color name of each color in the source palette is identified by the same color-naming model. By searching for the color with the smallest difference from the source color in the prototype palette with the same color name, the target color is obtained. Finally, the image is recolored based on the target palette to achieve color modification.

all the 11 color names, 'green', 'blue', and 'purple' have the highest counts, so we add an extra 5 colors for each of these 3 color names. Additionally, to ensure consistency in human skin tones in portraits, we also add 5 more colors for 'red' and 'pink'.

Up to this point, we have ensured that the colors in each prototype palette are of homogeneous color terms. Next, to guarantee a large saturation value from each constructed partition, we select the color with the highest saturation in the cluster as the candidate color for the prototype. Therefore, we end up with a prototype of candidate colors per color term $P^p = \{c_1^p, c_2^p, ..., c_n^p\}$, which have both stable color names and high saturation.

### B. Color Palette Extraction

For an input image, we extract a color palette $P^s = \{c_1^s, c_2^s, ..., c_l^s\}$ that represents the primary colors of the image. To reduce computational complexity, we first compute the color histogram of the image and extract the color palette $P^s$ by k-means clustering based on this histogram, where the cluster centers are selected as the colors in the palette. The color histogram is computed on *ab* channels in the *Lab* color space to avoid the influence of regions with excessively low or high lightness on the clustering results. In most cases, the number of the cluster center $l$ is typically set to a fixed value, with $l = 5$ being the most common choice in graphic design. However, since the richness of colors varies among different images, the optimal number of colors may vary for each image. To avoid an excessive number of similar colors in the palette, we determine the optimal number of clustering centers based on the percentage of explained variance [1]. For each value of $l$, ranging from 2 to 7, we calculate the within-group distortion. This involves the summation of the distance $d_l$ of each point in the cluster to its center. The total distortion $d_1$ is the summation of distances between each color point and the overall mean color. We select the optimal value of l when $\frac{d_1 - d_l}{d_1 - d_7} > \gamma$, with $\gamma = 0.93$.

TABLE I
COMPARISON OF IMAGE QUALITY AND HARMONY SCORE ON THE CAMERA RAW VERSION OF FIVEK [25], KODAK [26] AND PPR10K [27] DATASETS.
▨, ▨ INDICATE SMALLER AND LARGER VALUES ARE BETTER, RESPECTIVELY.) ▨, ▨ INDICATE THE BEST AND SECOND BEST RESULTS.

| Data | FiveK (Camera Raw) | | | | | PPR10K | | | | | Kodak | | | | |
|---|---|---|---|---|---|---|---|---|---|---|---|---|---|---|---|
| Metrics | NIQE | BRISQUE | F-score | MITS | PIT(%) | NIQE | BRISQUE | F-score | MITS | PIT(%) | NIQE | BRISQUE | F-score | MITS | PIT(%) |
| SRIE [28] | 3.32 | 41.09 | 1477 | 0.368 | 90.97 | 4.00 | 43.59 | 412 | 0.372 | 93.13 | 2.90 | 49.36 | 1104 | 0.320 | 91.86 |
| CURL [29] | 3.46 | 41.85 | 2841 | 0.44 | 87.93 | 4.24 | 46.32 | 928 | 0.419 | 90.30 | 3.06 | 51.58 | 1909 | 0.442 | 89.00 |
| DeepUPE [30] | 3.40 | 40.88 | 1502 | 0.399 | 91.38 | 4.09 | 45.23 | 318 | 0.408 | 94.55 | 3.08 | 51.93 | 895 | 0.371 | 92.52 |
| CLIP-LIT [31] | 3.36 | 44.18 | 1489 | 0.366 | 91.03 | 3.72 | 46.14 | 414 | 0.370 | 93.03 | 3.24 | 55.23 | 1100 | 0.319 | 91.77 |
| 3DLUT [32] | 3.48 | 41.98 | 2406 | 0.453 | 88.9 | 4.29 | 46.53 | 688 | 0.432 | 91.08 | 3.06 | 50.00 | 1674 | 0.465 | 88.70 |
| AdaInt [33] | 3.44 | 42.5 | 2379 | 0.455 | 89.21 | 4.20 | 45.60 | 671 | 0.446 | 90.48 | 3.07 | 49.87 | 1709 | 0.463 | 88.47 |
| C-Harmony [2] | 3.52 | 38.17 | 58 | 0.368 | 98.39 | 4.07 | 42.23 | 14 | 0.375 | 98.20 | 3.06 | 48.95 | 8 | 0.316 | 98.44 |
| Ours | 3.56 | 39.51 | 312 | 0.558 | 98.59 | 4.26 | 44.46 | 104 | 0.509 | 98.50 | 3.05 | 48.72 | 80 | 0.473 | 99.28 |

## C. Color Matching

This stage defines the target palette by selecting the best representative among the candidate colors for each color in the source color palette. To this end, given the RGB values of the source palette color, we run the color naming model and select possible colors for the target palette those in the prototype that share the same color name. Then, among all these colors, we choose the one that has the smallest difference to the source color as the target one. Here, we compute the RGB Euclidean distance for color distance measurement. Note that as there might be some source colors having similar probabilities of belonging to multiple color names, a relaxed search space is applied for the target color search. More in detail, instead of only getting the prototype colors for a single color term, we select the prototype colors for any color term that 1) has a probability greater than $15\%$, and 2) is among the top three color names in terms of probability.

## D. Palette-based Image Recoloring

Finally, we recolor the input image with the target palette. With the matched source and the target colors, color mapping is executed by inverse distance weighting, where larger weights are assigned to closer colors [1]. More specifically, given the pixel value of the input image $I^s$, source palette $P^s = \{c_1^s, c_2^s, ..., c_l^s\}$ and the corresponding target palette $P^t = \{c_1^t, c_2^t, ..., c_l^t\}$, the pixel in the recolored image $I^t$ with coordinate $(x, y)$ is determined by $I^t(x, y) = I^s(x, y) + \sum_{i=1}^{l} w_i(c_i^s - c_i^t)$, where the weight factor $w_i(x, y)$ is $w_i = \frac{1}{\sum_{i=1}^{l} |I^s(x,y) - c_i^s|^2 + \varepsilon}$, $\varepsilon = 10^{-4}$. The recolored image has higher saturation and a more distinct color for color naming.

## III. EXPERIMENTS

### A. Experimental Setup

**Datasets.** The MIT-Adobe FiveK dataset [34] contains 5,000 raw images taken with DSLR cameras, covering a broad range of scenes, subjects, and lighting conditions. We conduct experiments on the Camera Raw version of FiveK. The given DNG images are converted to 8-bit sRGB images with Adobe Photoshop using the Camera Raw software. For a fair comparison with deep learning-based approaches, we present the results of the test set, which is the last 500 images. The Kodak dataset [26] contains 24 8-bit sRGB images. The test images of FiveK and Kodak are resized with the shorter side set to 512 pixels. The Portrait Photo Retouching (PPR10K) dataset [27] contains 11,161 portrait photos. We use the validation split of the source 360p 16bit sRGB images and convert them to 8 bits required by the color naming model.

**Competing methods.** We compare our results versus recent deep-learning approaches, CURL [29], DeepUPE [30], 3DLUT [32], and AdaInt [33] that aim to minimize the difference from an expert photographer; an unsupervised deep-learning-based image enhancement approach, CLIP-LIT [31]; a traditional image enhancement method, SRIE [28]; and the color harmonization approach, C-Harmony [2].

**Image quality metrics.** Our image modification paradigm does not have any real ground-truth, since our goal is not to approximate the user intent, *e.g.* ExpertC in FiveK. We quantitatively evaluate the method by two non-reference image quality assessment metrics: NIQE [35] and BRISQUE [36]. These two metrics assess the perceptual naturalness of images.

**Color harmony metrics.** We evaluate color harmonious degree with three metrics: F-score [2], Mean Inside-Template Saturation (MITS), and Percentage of Inside-Template pixels (PIT). These metrics measure the color harmony of an image $I$ by comparing hue distribution $H$ and saturation $S$ with respect to a certain harmonious scheme $(m, \alpha)$, where $T_m$ is the template and $\alpha$ is the associated orientation. $x \in I_{in}$ and $x \in I_{out}$ indicate the pixels inside and outside the scheme, respectively. F-score is calculated as $F(I, (m, \alpha)) = \sum_{x \in I_{out}} \|H(x) - E_{T_m(\alpha)}(x)\| \cdot S(x)$, where $E_{T_m(\alpha)}(x)$ indicates the template border hue of $T_m(\alpha)$ that is closest to the hue of the pixel of the image. $\|H(x) - E_{T_m(\alpha)}(x)\|$ denotes the hue distance from a pixel to the nearest boundary of the harmonic scheme $T_m(\alpha)$, measured in radians, on the hue wheel. A smaller F-score indicates that there are fewer pixels with hues outside the template and that those out-of-template pixels have lower saturation. With the same optimal harmonious scheme found by F-score, we compute PIT that quantifies the proportion of pixels within the template: $PIT(I) = \frac{N(x \in I_{in})}{N(x \in I)}$, where $N()$ denotes the number of pixels that meet the specified criteria. MITS calculates the average saturation of pixels within the template: $MITS(I) = \frac{\sum_{x \in I_{in}} S(x)}{N(x \in I_{in})}$. Larger PIT and MITS suggest more pixels with higher saturation values inside the optimal template, respectively, therefore complementing the F-score metric.

Fig. 3. Comparison of images against other methods on FiveK. Our method produces more saturated colors while preventing unnatural color shifts.

## B. Quantitative Results

Table I looks at the results for three different datasets. It shows that for traditional blind quality assessment metrics (NIQE, BRISQUE), both our method and C-Harmony are competitive against traditional state-of-the-art enhancement models. It is important to remember that our goal is to not only obtain an image that is enhanced but also better in terms of its color scheme. Our method is the best for both MITS and PIT and second for F-score in these datasets, which indicates that our results exhibit a distribution that aligns more closely with the harmonic template and possesses higher saturation. Also, we should remark that C-Harmony [2] is optimized to minimize the F-score, the only one of the three harmonization metrics where it outperforms us. Also, since the image enhancement methods (SRIE, CURL, DeepUPE, CLIP-LIT, 3DLUT, and AdaInt) do not target to optimize color harmony, their performance on PIT is somehow lacking (90%), while our method and C-Harmony are over 98%.

## C. Qualitative Results

Compared to other methods, our approach does not produce over-illuminated images as CLIP-LIT [31] (in Fig. II-D), and artifacts in regions with high brightness, which happens in CURL and C-Harmony (see Fig. II-D and Fig. II-D). Additionally, in most cases, our approach increases image saturation while minimizing significant hue shifts, avoiding the unnatural color changes that sometimes occur in color harmonization methods (in Fig. II-D).

## D. Ablation study

In this subsection, we focus on the ablation study on the Camera Raw version of FiveK.

**Number of prototype colors.** The prototype palette determines the richness of colors in the recolored image. We, therefore, compare the differences in image quality and color harmonious score when varying the number of prototype colors, from 5 to 50 for each color name. Table II shows that as the number of prototype colors decreases, the color harmony-related metrics of the images improve. This is because, with a limited color palette, the color range of the recolored images

### TABLE II
### ABLATION OF THE NUMBER OF PROTOTYPE COLORS ON FIVEK.

| Number | Names | NIQE | BRISQUE | F-score | MITS | PIT(%) |
|--------|-------|------|---------|---------|------|--------|
| 5 | top1 | 3.573 | 39.374 | 987 | **0.643** | 97.01 |
| 10 | top1 | 3.564 | 39.668 | 890 | 0.608 | 96.95 |
| 15 | top1 | 3.559 | 38.842 | 1278 | 0.549 | 93.11 |
| 20 | top1 | 3.545 | 38.905 | 1699 | 0.530 | 91.87 |
| 50 | top1 | **3.531** | **38.654** | 1679 | 0.458 | 92.15 |
| 10+5 | top1 | 3.568 | 39.608 | 427 | 0.602 | 98.11 |
| 10+5 | top2 | 3.559 | 39.508 | 318 | 0.563 | 98.56 |
| 10+5 | top3 | 3.556 | 39.510 | **312** | 0.558 | **98.59** |

### TABLE III
### ABLATION OF COLOR SIMILARITY MEASURES ON FIVEK.

| Similarity | NIQE | BRISQUE | F-score | MITS | PIT(%) |
|------------|------|---------|---------|------|--------|
| Angular | 3.541 | **38.83** | 980 | 0.502 | 95.14 |
| Probability | **3.538** | 38.90 | 893 | 0.510 | 95.25 |
| Euclidean | 3.556 | 39.51 | **312** | **0.558** | **98.59** |

is constrained, making it easier to map different source colors to the same target color. With 10 prototype colors for each color name and 5 additional colors for the color name with the largest number of colors, most of the harmony metrics showed improvement. Moreover, these extra colors help reduce hue shifts to some extent, particularly in the case of skin tones.

**Color similarity measures.** We also compared different color similarity measurement methods, including Euclidean distance, angular distance [37], and color-naming probability similarity [23] for color matching. The first two directly measure color distance in the color space, while the latter assesses similarity in color-naming space by calculating cross-entropy between color probability distributions for different color names. Table III shows that the Euclidean distance-based method outperforms others in metrics related to color harmony.

## IV. CONCLUSION

This paper introduces a method for color harmonization based on color palettes and color naming. Our method is particularly well-suited for image modification in graphic design, where adhering to a color scheme is important. Experiments across multiple datasets help demonstrate the robustness and generalization ability of our method across diverse inputs.

## REFERENCES

[1] R. M. Nguyen, B. Price, S. Cohen, and M. S. Brown, "Group-theme recoloring for multi-image color consistency," in *Computer Graphics Forum*, vol. 36, no. 7. Wiley Online Library, 2017, pp. 83–92.

[2] D. Cohen-Or, O. Sorkine, R. Gal, T. Leyvand, and Y. Xu, "Color harmonization," *ACM Trans. Graph.*, vol. 25, no. 3, pp. 624–630, 2006.

[3] L. Shapira, A. Shamir, and D. Cohen-Or, "Image appearance exploration by model-based navigation," *Comput. Graph. Forum*, vol. 28, no. 2, pp. 629–638, 2009.

[4] Adobe, "Adobe color," https://color.adobe.com/, Accessed: 2023-08-04.

[5] S. Lin and P. Hanrahan, "Modeling how people extract color themes from images," in *ACM SIGCHI Conference on Human Factors in Computing Systems*, W. E. Mackay, S. A. Brewster, and S. Bødker, Eds. ACM, 2013, pp. 3101–3110.

[6] H. Chang, O. Fried, Y. Liu, S. DiVerdi, and A. Finkelstein, "Palette-based photo recoloring," *ACM Trans. Graph.*, vol. 34, no. 4, pp. 139:1–139:11, 2015.

[7] Q. Zhang, C. Xiao, H. Sun, and F. Tang, "Palette-based image recoloring using color decomposition optimization," *IEEE Trans. Image Process.*, vol. 26, no. 4, pp. 1952–1964, 2017.

[8] J. Tan, J. Lien, and Y. I. Gingold, "Decomposing images into layers via rgb-space geometry," *ACM Trans. Graph.*, vol. 36, no. 1, pp. 7:1–7:14, 2017.

[9] J. Tan, J. I. Echevarria, and Y. I. Gingold, "Efficient palette-based decomposition and recoloring of images via rgbxy-space geometry," *ACM Trans. Graph.*, vol. 37, no. 6, p. 262, 2018.

[10] J. Kang and Y. Hwang, "Hierarchical palette extraction based on local distinctiveness and cluster validation for image recoloring," in *IEEE International Conference on Image Processing*. IEEE, 2018, pp. 2252–2256.

[11] J. Tan, J. I. Echevarria, and Y. I. Gingold, "Palette-based image decomposition, harmonization, and color transfer," *CoRR*, vol. abs/1804.01225, 2018.

[12] H. Rahman and G. C. Paul, "Tripartite sub-image histogram equalization for slightly low contrast gray-tone image enhancement," *Pattern Recognit.*, vol. 134, p. 109043, 2023.

[13] M. V. Conde, F. Vasluianu, J. Vazquez-Corral, and R. Timofte, "Perceptual image enhancement for smartphone real-time applications," in *IEEE/CVF Winter Conference on Applications of Computer Vision*. IEEE, 2023, pp. 1848–1858.

[14] T. Wang, Y. Li, J. Peng, Y. Ma, X. Wang, F. Song, and Y. Yan, "Real-time image enhancer via learnable spatial-aware 3d lookup tables," in *IEEE/CVF International Conference on Computer Vision*. IEEE, 2021, pp. 2451–2460.

[15] X. Huo and J. Tan, "An improved method for color harmonization," in *International Congress on Image and Signal Processing*. IEEE, 2009, pp. 1–4.

[16] X. Li, H. Zhao, G. Nie, and H. Huang, "Image recoloring using geodesic distance based color harmonization," *Comput. Vis. Media*, vol. 1, no. 2, pp. 143–155, 2015.

[17] Y. Wan, Z. Tang, Z. Miao, and B. Li, "Image composition with color harmonization," *Int. J. Pattern Recognit. Artif. Intell.*, vol. 26, no. 3, 2012.

[18] Y. Baveye, F. Urban, C. Chamaret, V. Demoulin, and P. Hellier, "Saliency-guided consistent color harmonization," in *Computational Color Imaging - 4th International Workshop*, ser. Lecture Notes in Computer Science, S. Tominaga, R. Schettini, and A. Trémeau, Eds., vol. 7786. Springer, pp. 105–118.

[19] N. Sawant and N. J. Mitra, "Color harmonization for videos." in *Indian Conference on Computer Vision, Graphics and Image Processing*. Citeseer, 2008, pp. 576–582.

[20] B. Berlin and P. Kay, *Basic color terms: Their universality and evolution*. Univ of California Press, 1991.

[21] R. Benavente, M. Vanrell, and R. Baldrich, "Parametric fuzzy sets for automatic color naming," *JOSA A*, vol. 25, no. 10, pp. 2582–2593, 2008.

[22] C. A. Párraga, R. Benavente, M. Vanrell, and R. Baldrich, "Psychophysical measurements to model intercolor regions of color-naming space," *Journal of Imaging Science and Technology*, vol. 53, no. 3, p. 031106, 2009.

[23] J. Van De Weijer, C. Schmid, J. Verbeek, and D. Larlus, "Learning color names for real-world applications," *IEEE Trans. Image Process.*, vol. 18, no. 7, pp. 1512–1523, 2009.

[24] L. Yu, L. Zhang, J. van de Weijer, F. S. Khan, Y. Cheng, and C. A. Párraga, "Beyond eleven color names for image understanding," *Mach. Vis. Appl.*, vol. 29, no. 2, pp. 361–373, 2018.

[25] R. Liu, L. Ma, Y. Wang, and L. Zhang, "Learning converged propagations with deep prior ensemble for image enhancement," *IEEE Trans. Image Process.*, vol. 28, no. 3, pp. 1528–1543, 2018.

[26] E. Kodak, "Kodak lossless true color image suite," http://r0k.us/graphics/kodak/, 1999.

[27] J. Liang, H. Zeng, M. Cui, X. Xie, and L. Zhang, "PPR10K: A large-scale portrait photo retouching dataset with human-region mask and group-level consistency," in *IEEE Conference on Computer Vision and Pattern Recognition*. Computer Vision Foundation / IEEE, 2021, pp. 653–661.

[28] X. Fu, D. Zeng, Y. Huang, X. S. Zhang, and X. Ding, "A weighted variational model for simultaneous reflectance and illumination estimation," in *IEEE Conference on Computer Vision and Pattern Recognition*. IEEE Computer Society, 2016, pp. 2782–2790.

[29] S. Moran, S. McDonagh, and G. G. Slabaugh, "CURL: neural curve layers for global image enhancement," in *International Conference on Pattern Recognition*. IEEE, 2020, pp. 9796–9803.

[30] R. Wang, Q. Zhang, C. Fu, X. Shen, W. Zheng, and J. Jia, "Underexposed photo enhancement using deep illumination estimation," in *IEEE Conference on Computer Vision and Pattern Recognition*. Computer Vision Foundation / IEEE, 2019, pp. 6849–6857.

[31] Z. Liang, C. Li, S. Zhou, R. Feng, and C. C. Loy, "Iterative prompt learning for unsupervised backlit image enhancement," in *IEEE/CVF International Conference on Computer Vision*. IEEE, 2023, pp. 8060–8069.

[32] H. Zeng, J. Cai, L. Li, Z. Cao, and L. Zhang, "Learning image-adaptive 3d lookup tables for high performance photo enhancement in real-time," *IEEE Trans. Pattern Anal. Mach. Intell.*, vol. 44, no. 4, pp. 2058–2073, 2022.

[33] C. Yang, M. Jin, X. Jia, Y. Xu, and Y. Chen, "Adaint: Learning adaptive intervals for 3d lookup tables on real-time image enhancement," in *IEEE Conference on Computer Vision and Pattern Recognition*. IEEE, 2022, pp. 17 501–17 510.

[34] V. Bychkovsky, S. Paris, E. Chan, and F. Durand, "Learning photographic global tonal adjustment with a database of input / output image pairs," in *IEEE Conference on Computer Vision and Pattern Recognition*. IEEE Computer Society, 2011, pp. 97–104.

[35] A. Mittal, R. Soundararajan, and A. C. Bovik, "Making a "completely blind" image quality analyzer," *IEEE Signal Process. Lett.*, vol. 20, no. 3, pp. 209–212, 2013.

[36] A. Mittal, A. K. Moorthy, and A. C. Bovik, "No-reference image quality assessment in the spatial domain," *IEEE Trans. Image Process.*, vol. 21, no. 12, pp. 4695–4708, 2012.

[37] G. D. Finlayson and R. Zakizadeh, "Reproduction angular error: An improved performance metric for illuminant estimation," in *British Machine Vision Conference (BMVC)*. BMVA Press, 2014.